5A.4. Potentials of Frequency Agile Ka and W Band Cloud Radars

Valery Melnikov, Mark Yeary, Robert Huck, Redmond Kelley, Jess Phillips
University of Oklahoma, CIMMS and Atmospheric Radar Research Center, Norman, OK USA

INTRODUCTION

Vertically sounding radars at Ka and W bands are major instruments in cloud remote sensing. The use of short wavelengths make it possible to achieve a very high spatial resolution with relatively small antennas and provide good detectability of non-precipitating clouds. Reviews of ground-based cloud radars and their applications can be found in Kropfli and Kelly (1996), Kolias et al. (2007), and Shupe et al. (2008). Continuously running Millimeter wavelength Cloud Radars (MMCR), operated by the Atmospheric Radiation Measurement program, have vertically pointed beams so they can obtain cloud parameters above the radars. There are two types of MMCRs, the first operating at an 8-mm wavelength (Ka band; Moran et al., 1998; Hamazu et al., 2003), and the second at a 3-mm wavelength (W band; Widener and Mead, 2004; Manheimer et al., 2003). Retrieval of cloud parameters using MMCRs can be found in Kropfli and Kelly (1996); Clothiaux et al., (1995); Matrosov et al. (1992, 2002); and Reinking et al., (2002) among others.

Due to large variations in hydrometeors' properties in clouds and precipitations, measurements at a single wavelength are often ambiguous. To narrow the ambiguity, two wavelength and polarimetric measurements can be used. The latter are not so effective at vertical sounding because of scattering symmetry, although depolarization measurements can be used to distinguish between droplets and crystals and to remove clutter from insects and birds. Thus the proposed two-wavelength technique is an attractive approach, but requires two radars with collocated beams. Modern radars employ frequency agile transmitters. Therefore, it is attractive to implement these multi-wavelength methods with a single radar that is frequency agile. Some aspects of this approach at Ka and W bands are studied in this paper.

Largest droplet diameters in light rain lie in interval 0.5 to 3 mm and these sizes are comparable with the radar wavelengths at Ka and W bands, i.e., 8-mm and 3-mm respectively. Scattering properties for the bands are calculated using Mie theory. Measurements at these two wavelengths allow obtaining additional information on scattering media. Scattering resonance effects are quite strong at mm-wavelengths: even small deviations in ratios of the particle's diameter and wavelength can results in several dB deviation in the radar cross sections (section 3 herein). So the main goal of this paper is studying of effects of frequency changes within a band, i.e., the use of a two-wavelength techniques. The following questions are studied in this paper: 1) What frequency deviation is needed to produce measurable differences in returned power? 2) What information can be inferred from the power difference at two close wavelengths? 3) How strong are the deviations in the Doppler spectra at close wavelengths? These questions are studied for cloud radars at Ka and W bands.

The resonance scattering effects manifest themselves at long wavelengths such as X band and S band. At the 10-cm wavelength (S band), the effects are seen in scattering by large hailstones, birds, and insects (Melnikov et al., 2010a). Melnikov et al. (2010b) have shown that these effects should be observable in hail clouds at X-band as well. At mm-wavelengths, the resonance effects should manifest themselves for raindrops and cloud particles. Some aspects of these effects are considered in the next sections.

FREQUENCY AGILE RADARS FOR CLOUD SOUNDING

Frequency agile radars are used in weather observations to reduce the dwell time: measurements at different close wavelengths make the estimates at each wavelength independent which reduces the time of measurements (Bluestein et al., 2010, Wurman et al., 2010). In this paper, power differences for frequency agile radars at Ka and W bands are considered. Frequency agile radars with a klystron, travelling wave tube amplifier (TWTA), or solid state transmitters can generate signals within a wide frequency band. The waveguides can guide radiation at different frequencies within ±10% of its central frequency without substantial relative losses. So frequency chirping of 10% is considered herein.

Frequency agiling within a band is attractive for remote sensing since this allows multi-wavelength techniques to be implemented on a single radar. This also allows the elimination of some calibration difficulties since relative powers can be measured with an accuracy of about 0.3 dB. Secondly, at close wavelengths, attenuations in clouds and rain are about the same, which allows observations of the resonance effects more clearly than at quite different wavelengths. In other words, the resonance effect is measurable if a 10% frequency deviation produces a deviation in returned power larger than 0.3 dB.

A frequency agile radar operating at Ka band and designed at the University of Oklahoma is used. The bandwidth of this radar is from 30 to 36 GHz. Fig. 1 shows a picture of the front end of this portable Ka band radar that is currently under development. This prototype radar is housed in a shoebox size weatherproof box, which is not shown in Fig. 1. It is foreseeable that the shoebox radar will provide mobile remote sensing capabilities for a wide range of applications.

The portable radar transmits a continuous waveform composed of 30 to 36 GHz frequencies in steps of 10 MHz. The in-phase and quadrature (IQ) phase received signals are digitized by the data acquisition unit (DAQ). The DAQ connects the front end to a laptop computer via a serial communication channel, which allows the digitized IQ data to be uploaded. We propose the use of a laptop equipped with commercially available general purpose graphical processing units (GPGPU), where image formation processing can be implemented as a parallel process. This is attractive for any real time system where the same process such as a Fourier transform can be implemented on different data simultaneously.

RESONANCE EFFECTS AT CLOSE WAVELENGTHS

Consider first how strong the resonance effects at close wavelengths are for a distinct raindrop. Ka band and W band radiation with the wavelengths of 8-mm and 3-mm correspondingly are considered herein. A 10% increase in frequency results in 10% decrease of the wavelength; the results for two pairs of the wavelengths are presented: 8.0 and 7.2 mm at Ka band and 3.0 and 2.7 mm at W band. For small raindrops with diameters less than 0.5 mm, the backscatter cross sections σ can be calculated via the Rayleigh formulae (e.g., Bohren and Huffman, 1983, section 5.1)

$$\sigma_R = \frac{\pi^5 D^6}{\lambda^4}\left|\frac{\varepsilon-1}{\varepsilon+2}\right|^2, \qquad (1)$$

where λ is the wavelength, D is the diameter of a raindrop, ε is dielectric permittivity, and subscript 'R' signifies the Rayleigh approximation. Dielectric permittivity remains practically the same within a band so it can be considered constant. It follows from (1) that for the same scatterer, a small deviation $\Delta\lambda$ in the wavelength leads to a deviation in the cross section of

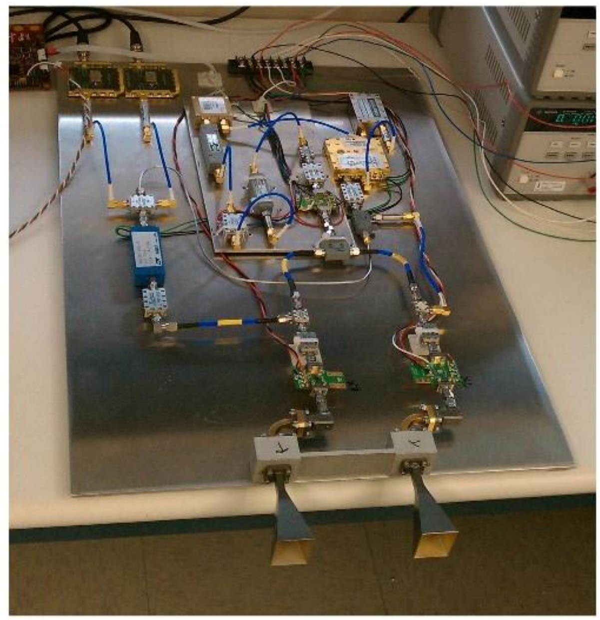

Fig. 1. The Ka band shoebox radar under development at the University of Oklahoma.

$-4\sigma_R\,\Delta\lambda/\lambda$. The relative alternation in the cross section is $1 - 4\Delta\lambda/\lambda$ which for a 10% deviation in frequency ($\Delta\lambda/\lambda = 0.1$) is 1.5 dB, i.e., a quite substantial value for measurements. But if the radar backscatter cross sections obey the Rayleigh law, no additional information on scattering media can be inferred from such changes in the scattered powers because such changes depend only on the deviation in wavelength and is the same for any scatterer. A new situation appears if droplets are not Rayleigh scatterers, which is the case at mm-wavelengths where σ should be calculated via the Mie formula (e.g., Bohren and Huffman, 1983, chapter 4, [16]). The ratio σ/σ_R shows the strength of deviations from the Rayleigh scattering regime.

In Fig. 2, σ/σ_R is shown as a function of drop diameter for the two pairs of wavelengths and for water temperature of 10^o C. Waviness of the curves manifests resonance effects that depend on the ratio $\pi D/\lambda$. One can see that the curves for the shorter wavelengths are shifted to the left from the curves for the longer wavelengths, i.e., the resonances occur at smaller particles. This shift leads to significant differences in backscatter cross-sections. It is also seen that the resonance effect becomes visible for raindrops larger than 1.7 mm at Ka band and for the ones larger than 0.7 mm at W band. The difference in received power with the same radar at close wavelengths can be measured with an accuracy of 0.3 dB. Fig. 2 also shows that the power difference for close wavelengths exceeds 0.3 dB in wide intervals of raindrop diameters, which means that the effects are measurable.

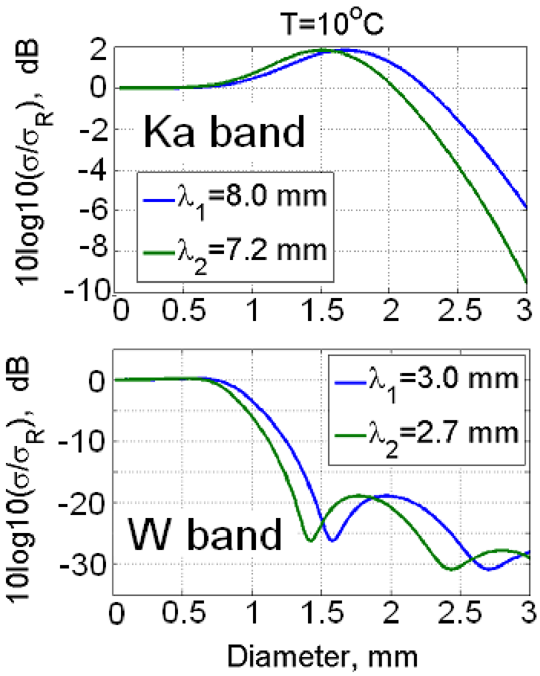

Fig. 2.Ratio of the backscatter cross sections of water drops via Mie and Rayleigh formulae for close wavelengths at Ka (top panel) and W (bottom panel) bands.

Natural rain contains droplets of different sizes. To quantify the resonance effects for light rain, we used the usual exponential drop size distributions (DSD),

$$N(D) = N_o \exp(D/D_o) \qquad (2)$$

where N_o and D_o are parameters. The third parameter of the DSD is the maximal size of droplets, D_{max}. It is known that in heavy rain, the maximal size of drops is 8 mm. In moderate and light rain, D_{max} is one of the main parameters which has to be obtained. In radar measurements, D_{max} is a very important parameter because the backscatter cross section is a strong function of the diameter.

To quantify the strength of the resonance effects in rain for close wavelengths, integration over the DSD (2) should be performed. Reflectivity Z is

$$Z(N_o, D_o, D_{max}) = \int_0^{D_{max}} \sigma(D)N(D)dD \qquad (3)$$

It is shown in (3) that measured reflectivity Z is a function of three parameters N_o, D_o, and D_{max}. Calculations of Z via (3) show that the difference in reflectivities for the close wavelength do not particularly depend on N_o and D_o if D_o is larger than 0.1 mm and is a function of D_{max}. The differences in Z are shown in Fig. 3 as functions of D_{max} which allows obtaining this parameter. One can see also that the reflectivity difference exceeds 0.3 dB for D_{max} larger than 1.5 and 0.7 mm at Ka and W bands correspondingly.

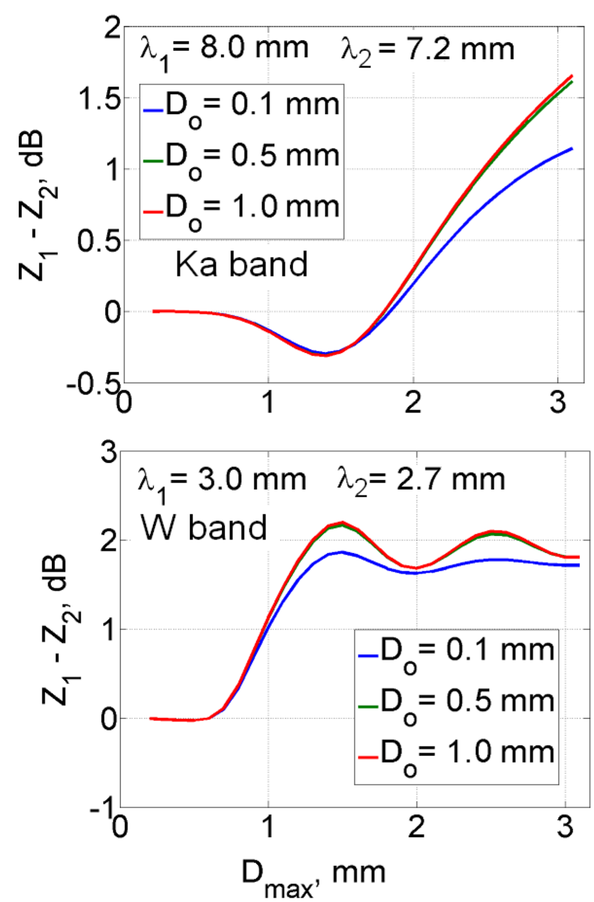

Fig. 3. Difference in reflectivities as a function of maximal drop diameter for Ka (top) and W (bottom) bands. The red and green lines practically coincide.

The reflectivity differences for ice/snow particles are quite different from those for rain. Fig. 3 depicts results for ice particles. Dielectric permittivity of solid ice was used in the calculations. By comparing Fig. 2 and Fig. 3 (the upper panels, Ka band) one can see substantial differences in values for diameters larger than 2 mm. Usually it is not difficult to delineate cloud regions with water and ice based on temperature profiles which are often known or from the location of the bright band seen in radar data. So the difference in reflectivities at close wavelengths could be used to estimate the maximal size of ice particles in clouds.

Uncertainties in the snow particles' densities could create uncertainties in D_{max} retrievals. This issue can be overcome with an analysis of the Doppler spectra obtained for the two close wavelengths.

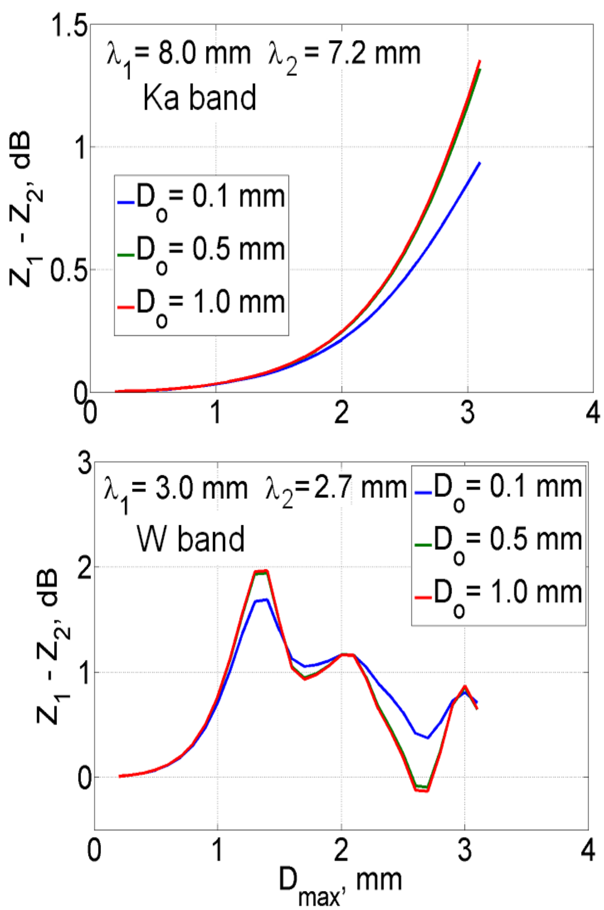

Fig. 4. Same as Fig. 3, but for ice particles.

At W band (the bottom panels in Figs. 2 and 3), the differences in reflectivities are almost the same for water droplets and ice particles with diameters smaller than 1.5 mm. For larger diameters, the reflectivity difference for water drops remains about 2 dB whereas for ice particles (Fig. 4) it drops down sharply to 1 dB at *D* about 1.5 - 2.0 mm and drops further down to 0 dB for *D* nearing 2.5 mm. By using a third wavelength that is different from 3.0 and 2.7 mm it is possible to obtain the maximal diameter of ice particles.

Calculated differences of reflectivities for two wavelengths at Ka band in rain are shown in Fig. 5. The size distribution is according to (2) from which one can see that the difference is a function of D_o and the frequency difference. The first frequency is 30 GHz at which reflectivity Z_1 is measured. The second frequency changes from 30 to 36 GHz as in the Ka band radar presented in Fig. 1. Reflectivity Z_2 is for the second frequency. It is seen from Fig. 5 that the measurement accuracy of 0.3 dB is sufficient to estimate D_o using two frequencies 30 and 36 GHz.

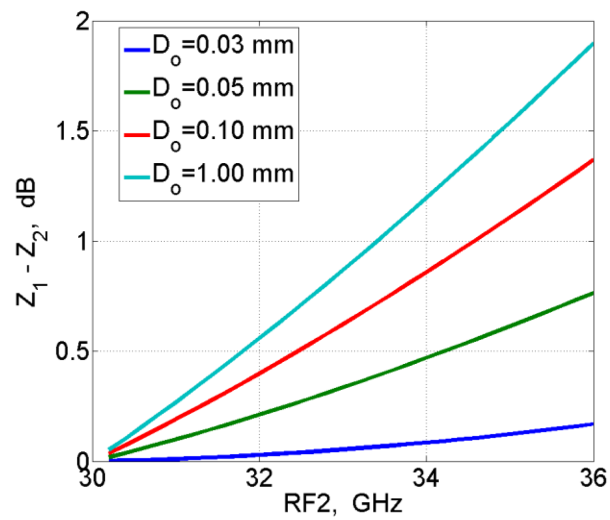

Fig. 5. Difference of reflectivity in rain with the size distribution (2) for two frequencies at Ka band: the first frequency is 30 GHz and the second one changes from 30 to 36 GHz.

Doppler Spectra at Close Wavelengths

Cloud radars at Ka and W bands sound vertically. In the absence of updrafts and downdrafts, the Doppler spectrum is determined by the falling particles' velocities which are a function of droplet size that allows obtaining their size distribution. Vertical air velocities and a strong horizontal wind make it difficult to separate their contributions from the contribution of the falling velocities. Strong horizontal winds widen the Doppler spectrum because of a finite antenna aperture. For instance, MMCR-3 with a 0.24° aperture width [6], horizontal winds of 25 m s^{-1} create 0.1 m s^{-1} spectral broadening which is comparable with usual spectral widths measured with the radar. So cloud updrafts/downdrafts and strong horizontal winds introduce uncertainties in DSD retrieval from the Doppler spectrum measured at a single wavelength. Measurements of the Doppler spectra at two close wavelengths eliminate influence of the mean wind velocities on the DSD retrievals.

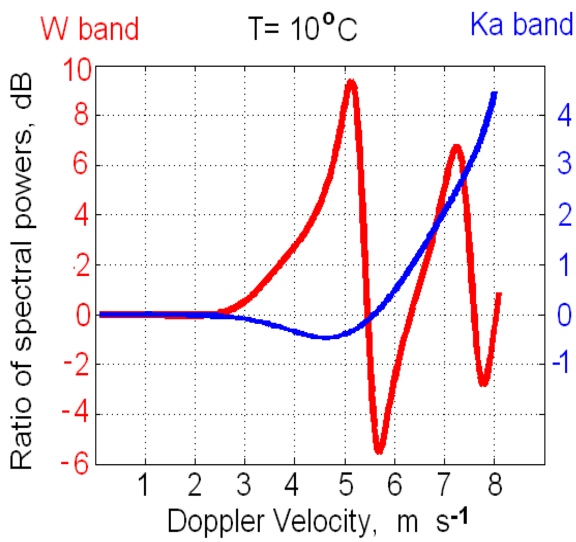

Fig. 6. Ratios of Doppler spectral powers at close wavelengths at Ka (blue) and W (red) bands. The power scales affiliated with Ka and W bands are highlighted with blue and red correspondingly.

In Fig. 6, the ratios of the spectral powers are shown for wavelengths of 3 and 2.7 mm (W band) and 8 and 7.2 mm (Ka band). It is seen that the ratios achieve several dB, i.e., these values are easily measurable. The ratios are independent from the mean wind in the radar volume and depend only on the difference in the close wavelengths. Using the spectral difference at close wavelengths, it is possible to obtain the DSD or alternatively three major parameters of the drop size distribution, N_o, D_o, and D_{max}.

Another advantage of the spectral ratios is that they do not depend on attenuation in precipitation, i.e., the spectral ratio can be used for radar volumes that located deep in scattering media. At a single wavelength, attenuation introduces uncertainties in retrievals. At two close wavelengths, attenuation is about the same but the resonance effects are strong.

CONCLUSIONS

Frequency agile Ka and W band radars allow implementing two-wavelength techniques with a single radar. Due to scattering resonance effects on cloud droplets it is possible to infer information on scattering particles by making measurements at two wavelengths within each band. We described a frequency agile Ka band radar with a bandwidth from 30 to 36 GHz.

The drop size distributions (DSD) in clouds are expressed with the exponential function with three parameters N_o, D_o, and D_{max} (see eq. (2)). Measurements of reflectivities at two wavelengths at Ka or W bands allow obtaining the maximum diameter D_{max} of droplets. 10% deviations in wavelengths within the bands are sufficient for such measurements.

Differences in the Doppler spectra obtained at vertical sounding at two wavelengths within the band allow obtaining the full DSD without any assumption about its shape. The spectral differences can reach several dB, i.e., they can be measured with high accuracies. Such measurements are not affected by the mean wind in the radar volume. Two-wavelength measurements implemented with frequency agile radars are less sensitive to attenuation of radiation in clouds and precipitation because resonance scattering effects are stronger than differences in attenuation.

REFERENCES

Bluestein, H.B., M. M. French, I. PopStefanija, and R. T. Bluth, 2010: Mobile, phased-array, X-band Doppler radar observations of tornadogenesis in the central U. S. 6th European Conference on Radar Meteorology, *ERAD-2010*, Sibiu, Romania, paper 10.1.

Bohren, C.F., and D.R. Huffman, 1983: *Absorption and Scattering of Light by Small Particles* , John Whilley and Son, San Diago, CA.

Clothiaux, E.E., et al., 1995: An evaluation of a 94-GHz radar for remote sensing of cloud properties. *J. Atmos. Oceanic Technol.*, **12**, 201-229.

Hamazu, K., H. Hashiguchi, T. Wakayama, T. Matsuda, R. J. Doviak, and S. Fukao, 2003: A 35-GHz scanning Doppler radar for fog observations. *J. Atmos. Oceanic Technol.*, **20**, 972-986.

Kollias, P., E. E. Clothiaux, M. A. Miller, B. A. Albrecht, G. L. Stephens, and T. P. Ackerman, 2007: Millimeter-wavelength radars: new frontier in atmospheric cloud and precipitation research. *Bull. Amer. Meteorol. Soc.*, 1608-1624.

Kropfli, R.A., and R.D. Kelly, 1996: Meteorological research applications of mm-wave radar. *Meteor. Atmos. Phys.*, **59**, 105–121.

Manheimer, W.M., et al., 2003: Initial cloud images with the NRL high power 94 GHz WARLOC radar. *Geophys. Res. Lett.*, **30**, 3, doi:10.1029/2002GL016507.

Matrosov, S.Y., T. Uttal, J. B. Snider, and R. A. Kropfli, 1992: Estimates of ice cloud parameters from ground-based infrared radiometer and radar measurements. J. *Geophys. Res.*, **97**, 11 567–11 574.

Matrosov, S.Y., A. Korolev, and A. J. Heymsfield, 2002: Profiling ice mass and characteristic particle size from Doppler radar measurements. *J. Atmos. Oceanic Technol.*, **19**, 1003–1018.

Melnikov, V.M., R. R. Lee, and N. J. Langlieb, 2010a: Hail reflectivity signatures from two adjacent WSR-88Ds: carrier frequency and calibration issues. *27th IIPS conference.* AMS, Phoenix, AZ, paper 8.5.

Melnikov, V., R. R. Lee, and N. J. Langlieb, 2010b: Resonance scattering at close wavelengths in hail and "clear air". 6th European Conference on Radar Meteorology, *ERAD-2010*, Sibiu, Romania, paper 2.4.

Moran, K., B. Martner, M. Post, R. Kropfil, D. Welsh, and K. Widener, "An unattended cloud-profiling radar for use in climate research," *Bulletin of the Amer. Met. Society*, vol. **79**, no. 3, pp. 443-455,1998.

Reinking, R.F., S. Y. Matrosov, R. A. Kropfli, and B.W. Bartram, 2002: Evaluation of a 45-slant quasi-linear radar polarization state for distinguishing drizzle droplets, pristine ice crystals, and less regular ice particles. *J. Atmos. Oceanic Technol*., **19**, 296-321.

Shupe, M.D., et al., 2008: A focus on mix phased clouds. The status of ground-based observational methods. *Bull. Amer. Meteorol. Soc.*, 1549-1562.

Widener, K.B., and J.B. Mead. 2004: W-band ARM cloud radar – Specifications and design. 15th ARM science team meeting Proceedings.

Wurman, J.K., K. Friedrich, K. Kosiba, 2010: Design and deployment of quickly scanning dual-frequency, dual-polarization, dual-Doppler mobile radar network. 6th European Conference on Radar Meteorology, *ERAD-2010*, Sibiu, Romania, paper 2.5.

.